A GRADED-MESH FDTD CODE FOR THE STUDY OF HUMAN EXPOSURE TO CELLULAR PHONES EQUIPPED WITH HELICAL ANTENNAS

P. Bernardi, M. Cavagnaro, S. Pisa, and E. Piuzzi

Department of Electronic Engineering, University "La Sapienza" of Rome
Via Eudossiana, 18, 00184 Rome, Italy

Abstract - **A FDTD code employing a graded mesh has been developed in order to make the FDTD technique suitable for studying cellular phones equipped with helical antennas. The graded-mesh FDTD allows the evaluation of both the radiating properties of the helical antenna, and the power absorption inside the user's head. First, a canonical case has been studied to find the optimal values for the grading factor "q" and the best model for approximating the circular wire section. It has been found that "q" values up to 3 can be used without introducing significant errors in the field solution, and that a good model for the wire circular section is a five-cell cross. Then, the free space radiating properties of a phone equipped with a helical antenna (radiation impedance, radiation pattern, etc) have been evaluated, and compared with those predicted by MoM, showing good agreement. Finally, the power absorption in an anatomical model of the human head has been computed for a radiated power of 250 mW at the frequency of 835 MHz. Peak SAR values of 0.98 W/kg averaged over 1 g and 0.63 W/kg averaged over 10 g have been obtained with the phone held in contact with the ear.**

I. Introduction

During the last years mobile telecommunication systems have experienced rapid growth. After the first generation of analog cellular phones, operating around 900 MHz with a radiated power of 600 mW, the second generation, based on digital systems, has entered the market. In particular, at present, one of the most widely used standards is the Global System for Mobile communication (GSM) in which the mobile terminal (MT) operates around 900 MHz and radiates a peak power of 2 W. However, due to the time division multiple access scheme employed, the MT transmits only for one eighth of the time, resulting in an average radiated power of 250 mW. This generation has now entered its second phase, represented by systems such as GSM 1800 in which the MT radiates an average power of 125 mW and operates around 1800 MHz [1]. Together with the above cited land mobile radio cellular system, satellite communication systems are also used. These systems work between 1.5 and 2.5 GHz for up and down links between the satellite and the MT, employing circular polarization [2].

In all these systems, the MT antenna plays a fundamental role. Some of the required characteristics are broad radiation patterns and enough bandwidth to allow real-time voice and data transmission. One possible antenna that satisfies these requirements is the helical antenna [3]-[8]. This antenna can provide wide-band impedance performance both with linear polarization, when operating in normal mode (i.e. the maximum radiation is in the plane normal to the antenna axis) for terrestrial links, and with circular polarization, when operating in axial mode (i.e. the maximum radiation is along the antenna axis) for satellite links.

An important issue in cellular telecommunication systems is the evaluation of the power deposition induced inside the user's head by the phone antenna. In [9], helical antennas operating in the normal mode were modeled within the FDTD method as a stack of electric and magnetic sources, and SAR induced in an anatomical model of the human head was evaluated. In [10], the effects that the proximity of a human head model has on the performance of a phone equipped with a helical antenna operating in axial mode have been studied. In order to fit the antenna geometry to the uniform 3-mm mesh used for the FDTD simulations, the antenna structure was modeled as a square helix using a staircase approximation. It must be noted that, by using the technique suggested in [9], the antenna radiation impedance can not be easily evaluated, while the approach presented in [10] does not allow an accurate simulation of the real antenna structure. The power deposition induced inside the user's head by a phone equipped with a helical antenna could be studied by using the FDTD technique with a very fine mesh. In this manner the helix geometry could be modeled with an adequate number of cells. Unfortunately this choice would give rise to huge memory occupation and long computation times. To overcome these problems a

graded-mesh FDTD code can be used. The graded mesh has been applied in literature to the modeling of the fine geometry of the ear in contact with a phone [11]-[13] and to the study of shielded or open waveguide structures [14]-[16].

In this paper the graded-mesh FDTD has been used to study the radiating properties of a phone equipped with a helical antenna and the power absorption in an anatomical model of the human head. In particular, for the simulation of the phone equipped with the helical antenna, a small cell size (0.3 mm) has been used in the region where the helix geometry must be modeled. Starting from this region, the cell size has been increased successively by a constant factor "q" (geometric series) up to the largest cell size (3 mm). In this manner, the phone radiation impedance can be directly evaluated as the ratio between the voltage and the current at the feed point, and the real helix geometry can be modeled with an adequate number of cells but with limited memory occupation.

II. Methods

The finite difference time domain (FDTD) numerical technique [17]-[19] has been used for computing the power deposition in a human head model due to a cellular phone. The head model has been obtained from a tissue-classified version of the "Visible Human Project" data set developed at Brooks Air Force Base laboratories [20]. The model has a total dimension of 63×83×85 cells with a 3-mm resolution, and discriminates 19 different types of tissues/organs. For the electrical characterization of the tissues at the frequencies of interest Gabriel's data [21] have been used.

A cellular phone model equipped with a helical antenna has been considered [see Fig. 1(a)]. The phone antenna operates in the normal mode at the frequency of 835 MHz, and it is realized with a wire of diameter equal to 1 mm. The diameter, the pitch, and the length of the helix are 4.2, 1.4, and 16 mm, respectively [9]. The dimensions of the metal case are 24×52×147 mm. The helix is mounted on the right-hand corner of this case in the far end with respect to the side of the earphone, and a straight metal connection of 20 mm in length is placed between the box and the helix. For comparison purposes, we have computed the characteristics of this phone in free space by using the freely available NEC implementation of the Method of Moments (MoM) [22]. This same phone has been also studied by considering the metal case covered with a plastic shell of thickness 3 mm and dielectric constant $\varepsilon_r = 2.7$.

A detail of the phone section parallel to the x-z plane and passing through the helix axis is reported in Fig. 1(b). The figure shows how the top of the case, the straight metal connection, and the lower part of the helix are reconstructed in the graded mesh.

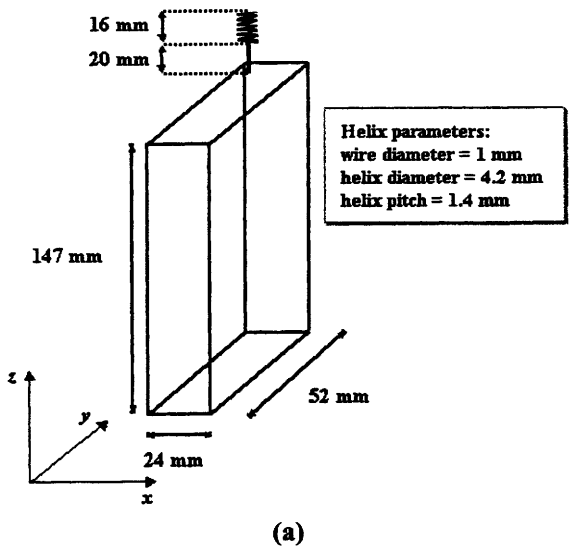

(a)

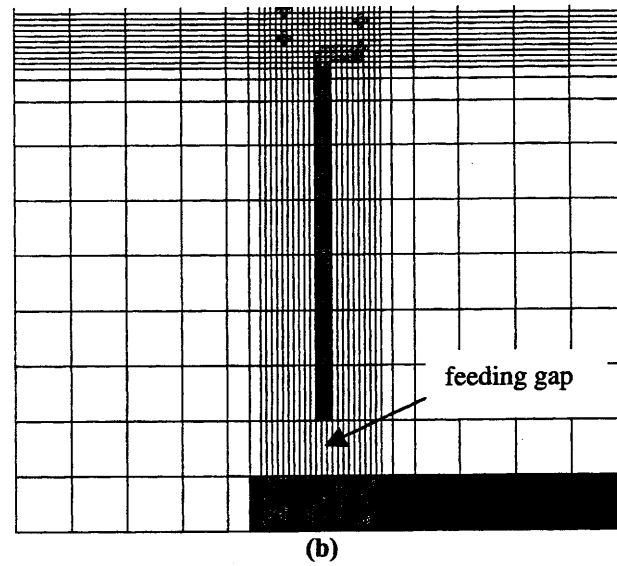

(b)

Fig. 1 (a) Cellular phone model considered (the plastic shell enclosing the metal case is not present). (b) Detail of the graded-mesh reconstruction of the phone section parallel to the x-z plane and passing through the helix axis (smallest cell size equal to 0.3 mm, largest cell size equal to 3 mm, grading factor equal to 2).

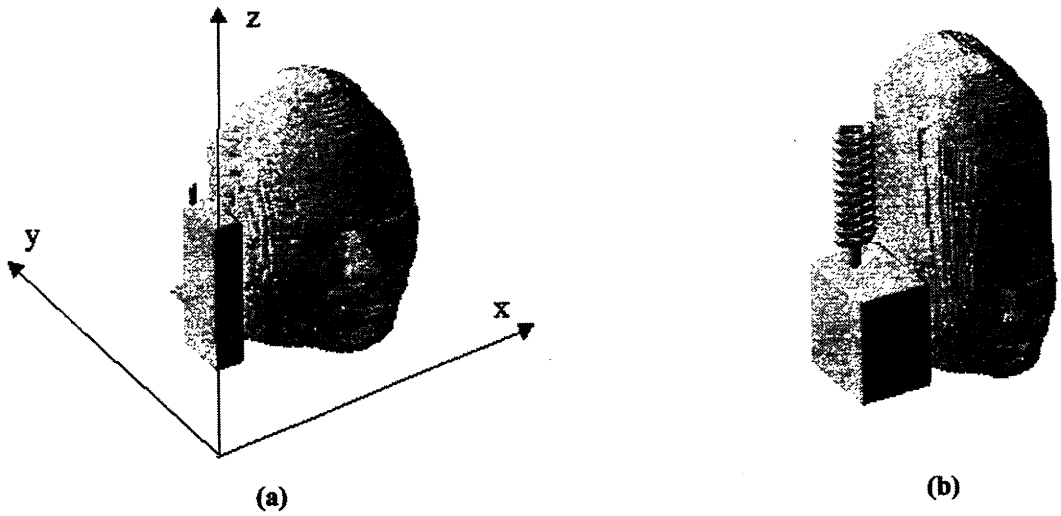

Fig. 2 Phone-head positioning in the (a) uniform and in the (b) graded mesh domain. Note that in Fig. 2(b) the entire geometry looks deformed due to the uniform representation of the graded mesh produced by the 3D visualization program.

In particular, for the graded mesh generation the following procedure has been adopted. First, the side lengths of the parallelepiped region to be studied are chosen taking into account the phone and head dimensions and the whole geometry of the problem. At the same time the center and the sides of the high-resolution region are fixed considering the position and dimensions of the helix. Then the size of the smallest cells (uniformly filling the high-resolution region) is chosen taking into account the smallest detail to be represented (typically the cross section of the helical wire), while the largest cell dimension is chosen considering the accuracy of the FDTD method that imposes the use of cell sizes not exceeding 1/10 of the wavelength at the highest frequency of interest. Finally, the graded sides $\delta_x(i)$, $\delta_y(j)$, $\delta_z(k)$ of the cells in which the domain is divided are determined assigning the smallest cell side to the cells filling the high resolution region and increasing the cell side outside this region with a given grading factor "q" till the largest cell side is reached. Once all the cell sizes are determined, the phone-head geometry is sampled in the resulting graded mesh. In particular, the helix is built filling with conductive material the cells placed around the helix analytical curve drawn in the FDTD grid. The result obtained applying this procedure to the previously described phone, kept in close contact with the head model, is shown in Fig. 2. In particular, Fig. 2(a) shows the real phone-head geometry, while Fig. 2(b) shows how this geometry is represented in the graded mesh (with cell sizes varying between 0.3 and 3 mm). In Fig. 2(b) the entire geometry looks deformed due to the uniform representation of the graded mesh produced by the 3D visualization program. The figure shows that a good model of the helix geometry is obtained by using the fine resolution of 0.3 mm.

The graded mesh domain has been bounded by using a four-cell uniaxial perfectly matched layer (UPML) absorbing boundary condition with parabolic profile and 1% reflection coefficient [19]. In all the simulations a gaussian pulse excitation has been applied at the antenna feed point [see Fig. 1(b)], and the simulation has been interrupted when the antenna feed current was reduced at least by three orders of magnitude with respect to the peak value. A soft E-field excitation has been used with a 50 Ω resistance placed in the feed point to simulate the generator internal impedance. The antenna radiation impedance has been computed as the ratio between the fast Fourier transforms of the voltage and current signals recorded at the feed point. The radiation pattern and the SAR distribution inside the head have been evaluated only at the operating frequency of 835 MHz through the discrete Fourier transform of the field components. The radiation pattern has been computed applying the near-to-far-field transformation [18].

III. Results

III.A Graded Mesh Optimization

In order to evaluate the optimum mesh-grading factor to be used in numerical simulations, the radiation impedance of a 16.6-cm long dipole has been studied at the resonant frequency of 900 MHz. The dipole has been inserted in a FDTD domain of 200×200×360 mm and has been modeled as a stack of cells both within a uniform grid of 2-mm side and within a graded mesh with cell sizes varying between 2 and 10 mm. In this last case different values for the grading factor "q" have been tested. In order to quantify the error due to the use of the graded mesh, the percentage error in the real and imaginary part of the radiation impedance (Z_R),

evaluated with the graded-mesh FDTD, with respect to those evaluated with the uniform mesh (Z_R = 95.02 + j51.28), has been considered. Fig. 3 shows the percentage errors for grading factors "q" ranging between 1 and 3. From the figure it appears that the error increases with "q", and for grading factors greater than 1.5 the error in the real part of the radiation impedance grows more rapidly than the error in the imaginary part. However, for all the grading factors considered the error is lower than 0.9%. For all the simulations that have been performed in this paper a value of 2 has been chosen for the grading factor "q". This choice is justified by the fact that for "q" = 2 the error is limited, and the memory occupation is significantly reduced with respect to the uniform mesh [23]. For the considered ratio between maximum and minimum cell size (10:2), using a grading factor greater than 2 would not yield any further reduction in memory occupation but would slightly increase the error.

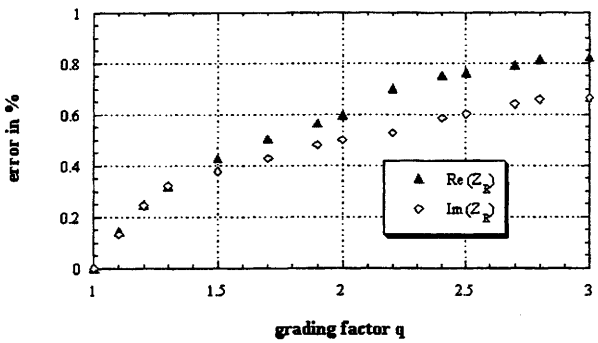

Fig. 3 Percent error in the real and imaginary part of the radiation impedance Z_R as a function of the "q" factor. Reference value: Z_R = 95.02 + j51.28.

Another important point is the choice of the cell configuration to be used for modeling the real circular section of the wire. To address this issue the 16.6-cm long dipole with cylindrical branches 2.26-mm in diameter (4-mm^2 section area) has been studied at the resonant frequency of 900 MHz. The dipole radiation impedance (Z_R) obtained by using MoM has been compared with that obtained by the graded-mesh FDTD considering different approximations of the wire cross section (Fig. 4).

The MoM-evaluated Z_R, used as reference value, is 94.21 + j45.77 Ω. Table I shows the Z_R values obtained with the graded-mesh FDTD using "q" = 2 and a five-cell cross [see Fig. 4(a)] for approximating the circular section. The different rows of table I correspond to different cell sizes employed in the high-resolution region where the dipole is built. The wire diameter is computed as the maximum distance between two points belonging to the wire section.

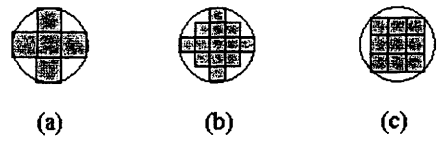

Fig. 4 Cell configuration for modeling the circular cross section of the wire: (a) five-cell cross; (b) thirteen-cell star; (c) nine-cell square.

TABLE I RADIATION IMPEDANCE VALUES OBTAINED WITH THE GRADED-MESH FDTD USING "q" = 2 AND A FIVE-CELL CROSS FOR APPROXIMATING THE CIRCULAR CROSS SECTION OF THE WIRE.

cell size [mm]	wire diameter [mm]	wire cross section [mm^2]	Re (Z_R) [Ω]	Im (Z_R) [Ω]
0.6	1.90	1.80	92.66	51.70
0.7	2.21	2.45	94.29	51.09
0.8	2.53	3.20	95.75	50.30
0.9	2.84	4.05	97.28	49.45
1.0	3.16	5.00	98.66	48.72
1.1	3.48	6.05	100.04	47.94

From the table it appears that the real part of Z_R, which is directly correlated to the power radiated by the phone, is closest to the MoM value for a cell size of about 0.7 mm, corresponding to a wire diameter of 2.21 mm and a section of 2.45 mm^2. Therefore, for a five-cell cross model of the wire section the best choice to reproduce the real part of Z_R is to choose a cross having a diameter equal to that of the real wire. Under this condition the error in the imaginary part of Z_R remains below 15%. Other cell configurations for the approximation of the wire section, such as a thirteen-cell star [see Fig. 4(b)] and a nine-cell square [see Fig. 4(c)], have been also tested. These configurations have been found to yield the same degree of accuracy as the cross, with the best approximation for the real part of Z_R obtained using once again a diameter equal to that of the real wire.

III.B Free-Space Analysis: Phone Model Validation

After these preliminary results, the free space radiation impedance and the radiation pattern for a realistic phone equipped with a helical antenna have been studied. The helical antenna considered is the one described in section II and is realized with a 1-mm diameter wire. This wire has been modeled, in the fine region of the graded mesh, with the five-cell cross. Following the indication of the previous analysis, the size of these cells has been chosen to be 0.3 mm. The largest cell size is 3 mm and the growing factor is 2. Fig. 5 shows, for this phone, the behavior of the real and imaginary parts of the radiation impedance as a function of frequency.

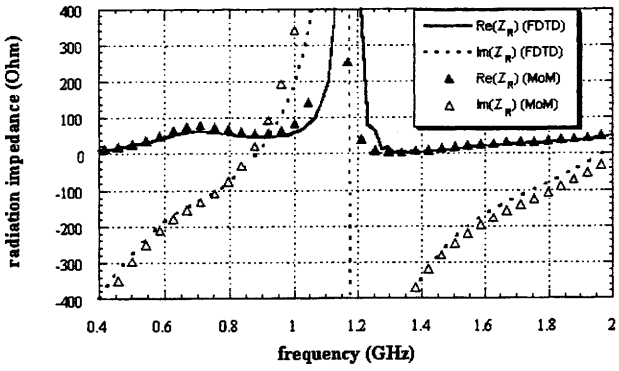

Fig. 5 Frequency behavior of the real and imaginary part of the antenna radiation impedance. The results obtained by using MoM are compared with those obtained with the graded-mesh FDTD technique for cell sizes varying between 0.3 and 3 mm with "q" = 2.

In the figure the results obtained with the graded-mesh FDTD technique are compared with those obtained with MoM. The values obtained with FDTD follow those predicted by MoM quite well. At the frequency of 835 MHz the error in the real part of the radiation impedance is about 18%. The highest errors are located around the first parallel resonance, while errors below 20% are found at the lower frequencies and around the first and the second series resonances. The phone bandwidth obtained at 835 MHz for a return loss better than 10 dB is about 7% evaluated both with MoM and FDTD.

The normalized radiation patterns at the frequency of 835 MHz on the z-y and x-y planes obtained by using the graded-mesh FDTD are reported in Fig. 6(a) and 6(b), respectively. The figure shows that the helical antenna operates in normal mode with a 30° down tilting and is almost omni-directional in the horizontal plane. On the same figure the results obtained for this phone by using the MoM are shown, and an excellent agreement between the two techniques is observed.

III.C SAR Evaluation

The interaction between the phone model with the metal case covered with plastic and the human head model has been studied at a frequency of 835 MHz and for a radiated power of 250 mW. Table II summarizes the main results of the simulations carried out for different positions of the phone. When the human head model is placed close to the phone, with the ear in contact with the case (first row), about 50% of the radiated power is absorbed inside the head. Peak SAR values of 0.98 and 0.63 W/kg averaged over 1 g and 10 g, respectively, are obtained. The peak SAR as averaged over 1 g is 0.2 W/kg in the brain, while it is only 0.011 W/kg in the eye.

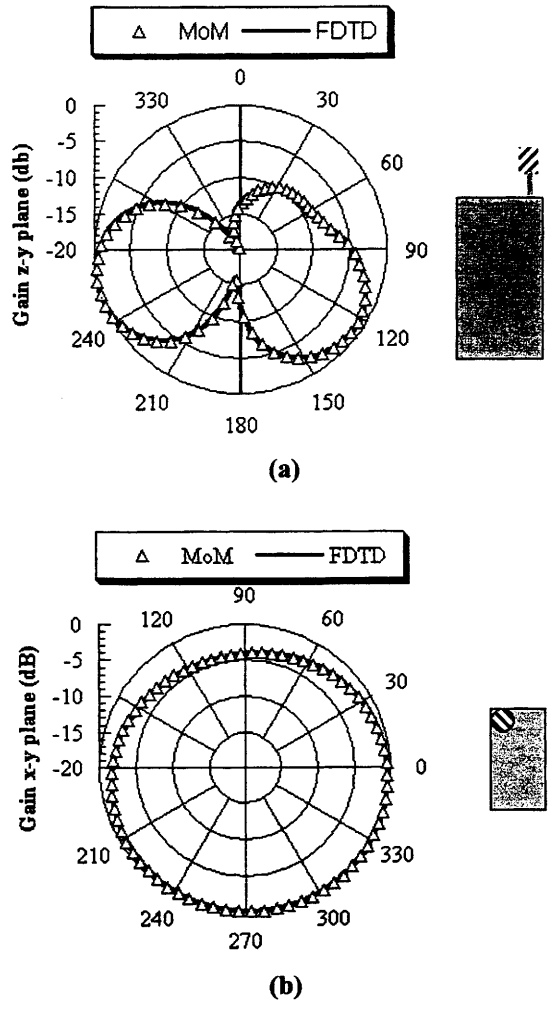

Fig. 6 Normalized radiation patterns of the phone in (a) the vertical plane and in (b) the horizontal plane. The results obtained by using the MoM method are compared with those obtained with the graded-mesh FDTD technique with "q" = 2.

If the phone is shifted by 3 mm towards the back of the head [y direction in Fig. 2(a)] the power and SAR values remain almost the same (see second row in table II). On the contrary, strong variations are observed when the phone is moved along the x direction in Fig. 2(a). In particular, when the phone is pressed against the ear, applying a 3-mm shift in the positive x-direction, the SAR as averaged over 1 g reaches 1.62 W/kg (third row in table II) and reduces to 0.55 W/kg when a 3-mm shift away from the ear is applied (fourth row in table II). Lower variations are observed in the peak SAR as averaged over 10 g and in the peak SAR in the brain and in the eye when the phone is moved towards and away from the ear (third and fourth row in table II).

TABLE II ABSORBED POWER AND SAR VALUES FOR VARIOUS PHONE POSITIONS (FREQUENCY: 835 MHz, RADIATED POWER: 250 mW).

	absorbed power [mW]	peak SAR 1g [W/kg]	peak SAR 10g [W/kg]	brain SAR 1g [W/kg]	eye SAR 1g [W/kg]
phone in contact with the ear	124	0.98	0.63	0.20	0.011
3-mm shift towards the head back	119	0.90	0.57	0.18	0.013
3-mm shift towards the ear	125	1.62	0.97	0.20	0.013
3-mm shift away from the ear	111	0.55	0.37	0.14	0.011
60° tilted phone in contact with the ear	108	0.86	0.49	0.12	0.009

The effect of phone tilting on SAR values, with the phone in contact with the ear, has been also studied. The tilting has been chosen to bring the bottom part of the phone case in front of the mouth, and this has been obtained leaving the phone in the vertical position and rotating the head in the forward direction by 60° [24]. The results obtained with the tilted phone are reported in the fifth row of table II. The comparison with the vertical position (first row in table II) shows a small reduction in the computed SAR values similar to that obtained shifting the phone towards the head back (see second row in table II). In [9], a SAR value of 1.35 W/kg averaged over 1 g was computed by using the same phone geometry and the same radiated power. Despite the differences in the head model, this value falls in the ranges obtained in the present work.

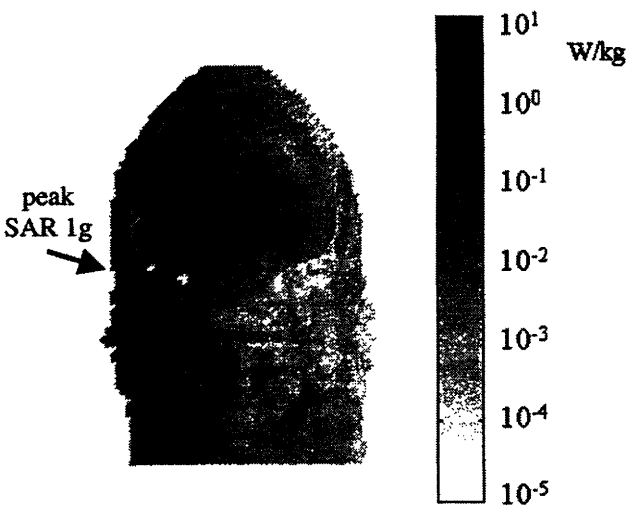

Fig. 7 SAR distribution on a vertical plane passing through the feed for a radiated power of 250 mW.

Finally, Fig. 7 shows the SAR distribution obtained on the vertical plane where the maximum SAR value is located, when the phone is kept in the vertical position and in contact with the ear. The highest SAR values are obtained in the middle of the ear where the phone case is in direct contact with the earlobe. Similar SAR patterns have been obtained in [25], [26].

IV. Conclusions

A graded-mesh FDTD code has been implemented for the study of phones equipped with helical antennas. The analysis of a canonical case has demonstrated that grading factors up to "q" = 3 can be used without introducing significant errors, but significantly reducing memory occupation, and that a good model for the circular cross section of the wire is a five-cell cross having the same diameter as the real wire.

The free space radiating properties of a commercial phone have been evaluated and compared with those computed with MoM, showing good agreement between the methods. The proposed technique has also proven effective for the assessment of the power absorption in the head of the user allowing the evaluation of the induced SAR distribution with an acceptable computational cost.

In particular, the technique has been used to study the influence on computed SAR values of the phone position and orientation. For a phone radiating a power of 250 mW at the frequency of 835 MHz peak SAR values lower than the limits suggested in international safety standards have been found when the phone is just touching the ear. A 65% increase in peak SAR values averaged over 1 g has been found when the phone is pressed hard against the ear.

It is worth noting that by using the graded mesh it has been possible to model the whole geometry of the above described problem employing only 2.3 millions of cells. This figure must be compared with the 927 millions of cells that would be required to solve the same problem employing a uniform mesh with 0.3-mm cell size, corresponding to the one adopted in the high resolution region.

Handheld units of satellite systems, employing helical antennas operating in axial mode, can also be studied with this technique [23]. In particular, both mono and quadrifilar antenna configurations can be easily modeled.

V. References

[1] ETSI, *Digital Cellular Telecommunication System, Radio Transmission and Reception (GSM 05.05)*, 1996.

[2] W.W. Wu, E.F. Miller, W.L. Pritchard, and R.L. Pickholtz, "Mobile satellite communications",

Proceedings of the IEEE, vol. 82, pp. 1431-1447, September 1994.

[3] J.D. Kraus, *Antennas*, 2nd ed. New York: Mc Graw-Hill, 1988.

[4] C.A. Balanis, *Antenna Theory: Analysis and Designs*, New York: Wiley, 1982.

[5] H. Nakano, Y. Samada, and J. Yamauchi, "Axial mode helical antennas", *IEEE Trans. on Antennas and Propagation*, vol. 34, pp. 1143-1148, September 1996.

[6] H. Nakano, N. Ikeda, Y.Y. Wu, R. Suzuki, H. Mimaki, and J. Yamauchi, "Realization of dual-frequency and wide-band VSWR performances using normal-mode helical and inverted-F antennas", *IEEE Trans. on Antennas and Propagation*, vol. 46, pp. 788-793, June 1998.

[7] J.S. Colburn and Y. Rahmat-Samii, "Quadrifilar-curl antenna for the big-LEO mobile satellite service system", in *IEEE Antennas Propagation Soc. Int. Symp.*, Baltimore, MD, vol. 2, pp. 1088-1091, July 1996.

[8] K.L. Virga and Y. Rahmat-Samii, "Efficient wide-band evaluation of mobile communication antennas using [Z] or [Y] matrix interpolation with the method of moment", *IEEE Trans. on Antennas and Propagation*, vol. 47, pp. 65-76, January 1999.

[9] G. Lazzi and O.P. Gandhi, "On modeling and personal dosimetry of cellular telephone helical antennas with the FDTD code", *IEEE Trans. on Antennas and Propagation*, vol. 46, pp. 525-530, April 1998.

[10] J.S. Colburn and Y. Rahmat-Samii, "Human proximity effects on circular polarized handset antennas in personal satellite communications", *IEEE Trans. on Antennas and Propagation*, vol. 46, pp. 813-820, June 1998.

[11] B.Q. Gao and O.P. Gandhi, "An expanding grid algorithm for the finite difference time domain method", *IEEE Trans. on Electromagnetic Compatibility*, vol. 34, pp. 277-283, August 1992.

[12] A. Tinniswood, G. Lazzi, and O.P. Gandhi, "The use of the expanding grid FDTD method for simulation of CAD derived personal wireless telephones", *Microwave and Optical Tech. Letters*, vol. 22, pp. 24-29, July 1999.

[13] J. Wiart, S. Chaillou, Z. Altman, and S. Drago, "Calculation of the power deposited in tissues close to a handset antenna using non-uniform FDTD", in *Electricity and Magnetism in Biology and Medicine*, Ed. by Bersani, Kluwer Academic/Plenum Publisher, pp. 717-720, 1999.

[14] V.J. Brankovic, D.V. Krupezevic, and F. Arndt, "An efficient two-dimensional graded mesh finite-difference time domain algorithm for shielded or open waveguide structures", *IEEE Trans. on Microwave Theory and Tech.*, vol. 40, pp. 2272-2277, December 1992.

[15] E.A. Navarro, T. Sangary, and J. Litva, "Some consideration on the accuracy of the nonuniform FDTD method and its application to waveguide analysis when combined with the perfectly matched layer technique", *IEEE Trans. on Microwave Theory and Tech.*, vol. 44, pp. 1115-1123, July 1996.

[16] W. Heinrich, K. Beilenhoff, P. Mezzanotte, and L. Roselli, "Optimum mesh grading for finite-difference method", *IEEE Trans. on Microwave Theory and Tech.*, vol. 40, pp. 1569-1574, September 1996.

[17] K. S. Kunz and R. J. Luebbers, *The Finite Difference Time Domain Method for Electromagnetics*, Boca Raton, FL: CRC Press, 1993.

[18] A. Taflove, *Computational Electrodinamics: the Finite-Difference Time-Domain Method*, Artech House, London, 1995.

[19] A. Taflove, *Advances in Computational Electrodinamics: the Finite-Difference Time-Domain Method*, Artech House, London, 1998.

[20] P.A. Mason, J.M. Ziriax, W.D. Hurt, T.J. Walters, K.L. Ryan, D.A. Nelson, K.I. Smith, and J.A. D'Andrea, "Recent advancements in dosimetry measurements and modeling", in *Radio Frequency Radiation Dosimetry*, B.J. Klauenberg and D. Miklavcic, Eds. Norwell, MA: Kluwer, 2000, pp. 141-155.

[21] C. Gabriel, "Compilation of the dielectric properties of body tissues at RF and microwave frequencies", *Brooks Air Force, Brooks AFB, TX, Tech. Rep. AL/OE-TR-1996-0037*, 1996 (see web site "http://www.fcc.gov/fcc-bin/dielec.sh").

[22] J. Burke and A. Poggio, *Numerical Electromagnetics Code (NEC) – Method of Moments*, Lawrence Livermore National Laboratory, Livermore, USA, Report No. UCID-18834, 1981.

[23] P. Bernardi, M. Cavagnaro, S. Pisa, and E. Piuzzi, "Evaluation of the power absorbed in a human head model exposed to cellular phones equipped with helical antennas", *Proc. 2000 IEEE MTT-S*, Boston, USA, pp. 1021-1024, June 2000.

[24] P. Bernardi, M. Cavagnaro, S. Pisa, and E. Piuzzi, "Specific absorption rate and temperature increases in the head of a cellular phone user", *IEEE Trans. on Microwave Theory and Tech.*, vol. 48, 7, pp. 1118-1126, July 2000.

[25] M. Okoniewski and M.A. Stuchly, "A study of the handset antenna and human body interaction", *IEEE Trans. Microwave Theory Tech.*, vol. MTT-44, pp. 1855-1864, October 1996.

[26] S. Watanabe, M. Taki, T. Nojima, and O. Fujiwara, "Characteristics of the SAR distributions in a head exposed to electromagnetic fields radiated by a hand-held portable radio", *IEEE Trans. Microwave Theory Tech.*, vol. MTT-44, pp. 1874-1883, October 1996.